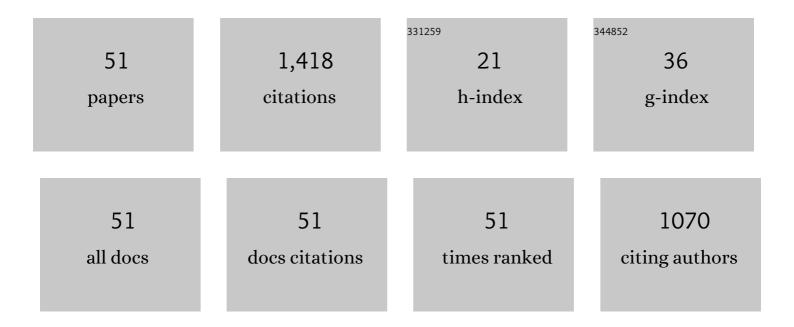
## **Baobao Chang**

List of Publications by Year in descending order

Source: https://exaly.com/author-pdf/7605550/publications.pdf Version: 2024-02-01



RAOBAO CHANC

#	Article	IF	CITATIONS
1	Creating anion defects on hollow CoxNi1-xO concave with dual binding sites as high-efficiency sulfur reduction reaction catalyst. Chemical Engineering Journal, 2022, 427, 132024.	6.6	13
2	lce template method assists in obtaining carbonized cellulose/boron nitride aerogel with 3D spatial network structure to enhance the thermal conductivity and flame retardancy of epoxy-based composites. Advanced Composites and Hybrid Materials, 2022, 5, 58-70.	9.9	105
3	Anion Doping for Layered Oxides with a Solid-Solution Reaction for Potassium-Ion Battery Cathodes. ACS Applied Materials & Interfaces, 2022, 14, 13379-13387.	4.0	11
4	In-situ synthesis of highly graphitized and Fe/N enriched carbon tubes as catalytic mediums for promoting multi-step conversion of lithium polysulfides. Carbon, 2022, 192, 418-428.	5.4	28
5	Environmentâ€tolerant conductive and superhydrophobic poly(mâ€phenylene isophthalamide) fabric prepared via γâ€ray activation and reduced graphene oxide/nano <scp>SiO<sub>2</sub></scp> modification. Journal of Applied Polymer Science, 2022, 139, .	1.3	3
6	High-Performance Gel Polymer Electrolyte with Self-Healing Capability for Lithium-Ion Batteries. ACS Applied Energy Materials, 2022, 5, 5267-5276.	2.5	14
7	Mechanically robust and conductive poly(acrylamide) nanocomposite hydrogel by the synergistic effect of vinyl hybrid silica nanoparticle and polypyrrole for human motion sensing. Advanced Composites and Hybrid Materials, 2022, 5, 2834-2846.	9.9	46
8	A facile and high-effective oxygen defect engineering for improving electrochemical performance of lithium-rich manganese-based cathode materials. Journal of Power Sources, 2022, 536, 231456.	4.0	25
9	One-Step Synthesis of PVDF-HFP/PMMA-ZrO <sub>2</sub> Gel Polymer Electrolyte to Boost the Performance of a Lithium Metal Battery. ACS Applied Energy Materials, 2022, 5, 7317-7327.	2.5	15
10	Design and Preparation of NiCoMn Ternary Layered Double Hydroxides with a Hollow Dodecahedral Structure for High-Performance Asymmetric Supercapacitors. ACS Applied Energy Materials, 2022, 5, 6772-6782.	2.5	22
11	Rational architecture design of yolk/double-shells Si-based anode material with double buffering carbon layers for high performance lithium-ion battery. Green Energy and Environment, 2021, 6, 517-527.	4.7	21
12	The retardation effects of lamellar slip or/and chain slip on void initiation during uniaxial stretching of oriented iPP. Polymer, 2021, 215, 123342.	1.8	4
13	Titanium Glycolate Nanorods with Unsaturated Sites as Multifunctional Layers for Advanced Lithium–Sulfur Batteries. ACS Applied Energy Materials, 2021, 4, 3670-3680.	2.5	5
14	Enhancing Reaction Kinetics of Sulfur-Containing Species in Li-S Batteries by Quantum Dot-Level Tin Oxide Hydroxide Catalysts. ACS Applied Energy Materials, 2021, 4, 4935-4944.	2.5	6
15	Tailoring bulk Li+ ion diffusion kinetics and surface lattice oxygen activity for high-performance lithium-rich manganese-based layered oxides. Energy Storage Materials, 2021, 37, 509-520.	9.5	55
16	Li <sub>2</sub> S In Situ Grown on Three-Dimensional Porous Carbon Architecture with Electron/Ion Channels and Dual Active Sites as Cathodes of Li–S Batteries. ACS Applied Materials & Interfaces, 2021, 13, 32968-32977.	4.0	11
17	Improving the Cycling Stability of Li-Rich Mn-Based Cathodes through Surface Modification of VOPO <sub>4</sub> . Energy & amp; Fuels, 2021, 35, 14148-14156.	2.5	9
18	Fe, Co-bimetallic doped C3N4 with in-situ derived carbon tube as sulfur host for anchoring and catalyzing polysulfides in lithium-sulfur battery. Journal of Alloys and Compounds, 2021, 873, 159883.	2.8	21

BAOBAO CHANG

#	Article	IF	CITATIONS
19	Encapsulating Nanoscale Silicon inside Carbon Fiber as Flexible Self-Supporting Anode Material for Lithium-Ion Battery. ACS Applied Energy Materials, 2021, 4, 8529-8537.	2.5	24
20	Simple Approach to Fabricate an Anisotropic Wetting Surface with High Adhesive Force toward Droplet Transfer. ACS Applied Polymer Materials, 2021, 3, 4470-4477.	2.0	1
21	Preparation and Performance of Eu <sup>3+</sup> -Doped BaSnF <sub>4</sub> -Based Solid-State Electrolytes for Room-Temperature Fluoride-Ion Batteries. ACS Sustainable Chemistry and Engineering, 2021, 9, 12978-12989.	3.2	5
22	Strain dependent crystallization of isotactic polypropylene during solid-state stretching. Polymer Testing, 2021, 104, 107404.	2.3	7
23	The Synergistic Effect of Rareâ€Earth Complex Nucleating Agent and Graphene Oxide on the Nonâ€Isothermal Crystallization Behavior of iPP Originating From the Diverse Selfâ€Assembly Morphology. Macromolecular Chemistry and Physics, 2021, 222, 2000357.	1.1	6
24	Boosting Electrochemical Performance of Lithium-Rich Manganese-Based Cathode Materials through a Dual Modification Strategy with Defect Designing and Interface Engineering. ACS Applied Materials & Interfaces, 2021, 13, 53974-53985.	4.0	28
25	Atomically Dispersed and O, N-Coordinated Mn-Based Catalyst for Promoting the Conversion of Polysulfides in Li <sub>2</sub> S-Based Li–S Battery. ACS Applied Materials & Interfaces, 2021, 13, 54113-54123.	4.0	9
26	Design and Facile Synthesis of Highly Efficient and Durable Bifunctional Oxygen Electrocatalyst Fe–N <sub><i>x</i></sub> /C Nanocages for Rechargeable Zinc-Air Batteries. ACS Applied Materials & Interfaces, 2021, 13, 54032-54042.	4.0	14
27	Influence of crystal orientation on stretching induced void formation in poly(4â€methylâ€1â€pentene) investigated by inâ€situ smallâ€angle and wideâ€angle <scp>Xâ€</scp> ray scattering. Polymer Crystallization, 2021, 4, e10215.	0.5	0
28	Insight into the Supercapacitive Behavior of Activated Hollow Porous Carbon Spheres in Different Electrolytes. ACS Applied Energy Materials, 2021, 4, 13766-13775.	2.5	4
29	Rapid sintering method for highly conductive Li7La3Zr2O12 ceramic electrolyte. Ceramics International, 2020, 46, 10917-10924.	2.3	146
30	Porous silicon–graphene–carbon composite as high performance anode material for lithium ion batteries. Journal of Energy Storage, 2020, 27, 101075.	3.9	31
31	Suppressing H2–H3 phase transition in high Ni–low Co layered oxide cathode material by dual modification. Journal of Materials Chemistry A, 2020, 8, 21306-21316.	5.2	112
32	Recent progress on germanium-based anodes for lithium ion batteries: Efficient lithiation strategies and mechanisms. Energy Storage Materials, 2020, 30, 146-169.	9.5	80
33	Preparation and performances of the modified gel composite electrolyte for application of quasi-solid-state lithium sulfur battery. Chemical Engineering Journal, 2020, 389, 124300.	6.6	60
34	Spherical Gr/Si/GO/C Composite as High-Performance Anode Material for Lithium-Ion Batteries. Energy & Fuels, 2020, 34, 7639-7647.	2.5	39
35	Improving the Structure and Cycling Stability of Ni-Rich Layered Cathodes by Dual Modification of Yttrium Doping and Surface Coating. ACS Applied Materials & Interfaces, 2020, 12, 19483-19494.	4.0	91
36	Sodium phthalate as an anode material for sodium ion batteries: effect of the bridging carbonyl group. Journal of Materials Chemistry A, 2020, 8, 8469-8475.	5.2	23

BAOBAO CHANG

#	Article	IF	CITATIONS
37	Hierarchically structured spherical nickel cobalt layered double hydroxides particles grown on biomass porous carbon as an advanced electrode for high specific energy asymmetric supercapacitor. Journal of Energy Storage, 2020, 30, 101454.	3.9	45
38	Flower-like ZnO modified with BiOI nanoparticles as adsorption/catalytic bifunctional hosts for lithium–sulfur batteries. Journal of Energy Chemistry, 2020, 51, 21-29.	7.1	30
39	Tellurium Surface Doping to Enhance the Structural Stability and Electrochemical Performance of Layered Ni-Rich Cathodes. ACS Applied Materials & Interfaces, 2019, 11, 40022-40033.	4.0	85
40	Competition effect of shearâ€induced nuclei and multiwalled carbon nanotubes (MWCNT) on βâ€isotactic polypropylene ( <i>i</i> PP) formation in preshear injectionâ€molded <i>i</i> PP/MWCNT nanocomposites. Polymer Composites, 2018, 39, E1149.	2.3	6
41	Influence of nucleating agent self-assembly on structural evolution of isotactic polypropylene during uniaxial stretching. Polymer, 2018, 138, 329-342.	1.8	29
42	Microstructure characterization in a single isotactic polypropylene spherulite by synchrotron microfocus wide angle X-ray scattering. Polymer, 2018, 142, 387-393.	1.8	6
43	Cavitation Behavior of Semi-Crystalline Polymers during Uniaxial Stretching Studied by Synchrotron Small-Angle X-Ray Scattering. , 2018, , .		0
44	Accelerating shear-induced crystallization and enhancing crystal orientation of isotactic-polypropylene via nucleating agent self-assembly. Polymer, 2018, 158, 213-222.	1.8	15
45	Critical Strains for Lamellae Deformation and Cavitation during Uniaxial Stretching of Annealed Isotactic Polypropylene. Macromolecules, 2018, 51, 6276-6290.	2.2	35
46	Influence of Annealing on Mechanical α <sub>c</sub> â€Relaxation of Isotactic Polypropylene: A Study from the Intermediate Phase Perspective. Macromolecular Materials and Engineering, 2017, 302, 1700291.	1.7	9
47	Microstructural Evolution of <i>Isotactic</i> â€Polypropylene during Creep: An In Situ Study by Synchrotron Smallâ€Angle Xâ€Ray Scattering. Macromolecular Materials and Engineering, 2017, 302, 1700152.	1.7	9
48	Tailoring microstructure and mechanical properties of injection molded isotactic–polypropylene via high temperature preshear. Polymer Engineering and Science, 2015, 55, 2714-2721.	1.5	9
49	Pre-shear induced anomalous distribution of β-form in injection molded iPP. Polymer Testing, 2013, 32, 545-552.	2.3	23
50	Enhanced βâ€crystal formation of isotactic polypropylene under the combined effects of acidâ€corroded glass fiber and preshear. Polymer Composites, 2013, 34, 1250-1260.	2.3	15
51	Engineering Si-Based Anode Materials with Homogeneous Distribution of SiO <sub><i>x</i></sub> and Carbon for Lithium-Ion Batteries. Energy & Fuels, 0, , .	2.5	8